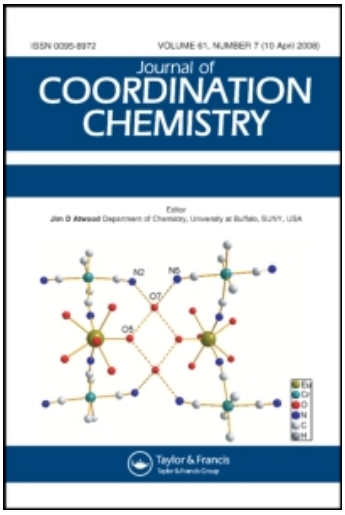


**Journal of Coordination Chemistry**
Publication details, including instructions for authors and subscription information:
http://www.informaworld.com/smpp/title~content=t713455674

# A POLYMERIC COMPLEX OF MANGANESE(II) AZIDE CONTAINING ALTERNATE END-ON AND END-TO-END BRIDGING AZIDO LIGANDS Synthesis, Structural, Spectroscopic and Thermal Study of $[Mn(N_3)_2$ (Ethyl Nicotinate)$_2]_n$

Mohamed A. S. Goher[a]; Najeeb A. Al-salem[a]; Franz A. Mautner[b]
[a] Department of Chemistry, Faculty of Science, Kuwait University, Safat, Kuwait [b] institut fur Physikalische und Theoretische Chemie, Technische Universitat Graz, Graz, Austria

**To cite this Article** Goher, Mohamed A. S. , Al-salem, Najeeb A. and Mautner, Franz A.(1998) 'A POLYMERIC COMPLEX OF MANGANESE(II) AZIDE CONTAINING ALTERNATE END-ON AND END-TO-END BRIDGING AZIDO LIGANDS Synthesis, Structural, Spectroscopic and Thermal Study of $[Mn(N_3)_2$ (Ethyl Nicotinate)$_2]_n$', Journal of Coordination Chemistry, 44: 1, 119 — 131
**To link to this Article: DOI:** 10.1080/00958979808022886
**URL:** http://dx.doi.org/10.1080/00958979808022886

*J. Coord. Chem.*, 1998, Vol. 44, pp. 119–131
Reprints available directly from the publisher
Photocopying permitted by license only





# A POLYMERIC COMPLEX OF MANGANESE(II) AZIDE CONTAINING ALTERNATE END-ON AND END-TO-END BRIDGING AZIDO LIGANDS

## Synthesis, Structural, Spectroscopic and Thermal Study of $[Mn(N_3)_2$ (Ethyl Nicotinate)$_2]_n$

MOHAMED A.S. GOHER[a*], NAJEEB A. Al-SALEM[a] and FRANZ A. MAUTNER[b]

[a]*Department of Chemistry, Faculty of Science, Kuwait University P.O. Box 5969 Safat, 13060 Kuwait;* [b]*Institut fur Physikalische und Theoretische Chemie, Technische Universitat Graz, A-8010 Graz, Austria*

*(Received 10 December 1996; Revised 1 April 1997; In final form 22 September 1997)*

A mixed ligand 1:2 manganese(II) azido complex of ethyl nicotinate has been synthesized and characterized by spectroscopic and crystallographic methods. The structure consists of a two-dimensional manganese-azido compound with each manganese atom in a *trans* octahedral environment, bonded to four azido ligands [Mn-N = from 2.199(4) Å to 2.231(3) Å] and two axial ethyl nicotinate ligands [Mn-N = 2.285(3) and 2.308(3) Å]. Two azido ligands are coordinated end-on between the manganese atoms giving planar and centrosymmetric $Mn_2N_2$ units. Each $Mn_2N_2$ unit is linked to four neighboring $Mn_2N_2$ units by means of four end-to-end azido bridges. The IR and Raman spectra correlate with the structure of the complex. The vibrational bands are compared with those of the free ligand. The EPR spectra of polycrystalline powder and solutions of the complex are measured at room temperature and discussed. The thermal decomposition of the complex was investigated derivatographically under nitrogen.

*Keywords:* ethyl nicotinate; azido; manganese(II) complex; thermal; crystal structure; spectra

The number of first row polynuclear complexes in which the paramagnetic centers, *e.g.*, copper[1] and nickel[2] are linked by means of azido ligands, has markedly increased in the past few years as a result of the fact that the magnetic behaviour of the azido systems changes with the coordination mode of the ligand.

*Author for correspondence.

End-to-end coordinated azide gave from moderate to very strong antiferromagnetic coupling[3-6], whereas end-on coordination generally gave ferromagnetic coupling[7-10]. The nuclearity of the polynuclear compounds is frequently greater than two. The manganese-azido system, on the other hand, has been poorly explored to date and the few reported compounds show a variety of dimensionality and magnetic behaviour. We have reported the monomeric compound $[Mn(quind)(N_3)(H_2O)]\cdot H_2O$ (quind = quinaldic acid)[11], the complex $[NaMn(pyz)(N_3)_2(H_2O)_2]$ (pyz = 2-pyrazinic acid), which is the first structurally characterized 1,1-azido dinuclear manganese compound[12], the two dimensional compound $[Mn(pic)(N_3)(H_2O)]$ (pic = picolinate), which contains carboxylato-manganese $Mn_2O_2$ units linked to four neighboring $Mn_2O_2$ units by means of four end-to-end azido bridges[13], and the three-dimensional $[Mn(pyridine)_2(N_3)_2]_n$ system[14]. Recently, Rojo *et al.* reported the structure and magnetic characterization of the dimeric $(\mu\text{-}N_3)_2[Mn(terpy)_2]_2(X_2)$ (terpy = terpyridine)[15] and the ferro-antiferromagnetic alternating chain $[Mn(bpy)(N_3)_2]$ (bpy = bipyridine)[16].

In the present study we describe the synthesis and structural characterization of a polymeric 1:2 complex of manganese(II) azide with ethyl nicotinate containing alternate end-on and end-to-end bridging azido ligands, elucidated by crystallographic and spectroscopic methods. The thermal properties of the complex are also described.



## EXPERIMENTAL

Ethyl nicotinate was purchased from Aldrich and the other chemicals were of analytical grade quality.

### Preparation of $[Mn(N_3)_2(\text{ethyl nicotinate})_2]_n$ Complex

An aqueous solution of $NaN_3$ (0.455 g, 7.0 mmol) was added dropwise to a mixture of an aqueous solution of manganese(II) chloride trihydrate (0.59 g, 3 mmol) and 30 mL of ethanolic solution of ethyl nicotinate (1.5 g, 10 mmol). The final clear solution was kept in a refrigerator for several weeks to produce colorless fine crystals of the complex. The fine crystals were filtered off and then dissolved in hot water. The filtrate was allowed to stand in a refrigerator over several weeks to produce pale yellow crystals with a tint of green color. These crystals were suitable for X-ray diffraction measurements. Anal. Calcd (%): C, 43.55; H, 4.10; N, 25.38; Mn, 12.24. Found: C, 43.7; H, 4.2; N, 25.3; Mn, 12.4.

## Physical Measurements

Raman spectra were obtained using a Perkin-Elmer System 2000 NIR FT-Raman spectrometer. The power of the laser beam used was approximately 80 mW. IR spectra were obtained using a Bruker IFS-25 model FT-IR spectrophotometer. Solid samples were measured as KBr pellets and liquid ligand as a capillary film. The experimental procedures and instruments used for other measurements are as described previously[17].

## X-ray Crystallography

A modified STOE four-circle diffractometer was used for single crystal X-ray measurements. Orientation matrix and lattice parameters were obtained by least-squares refinement of the diffraction data from 47 reflections in the 2θ range 10-26°. Data were collected at 295(2) K using graphite crystal-monochromatized Mo-K$\alpha$ radiation ($\lambda$ = 0.71069 Å) and the $\omega$-scan technique. The intensities were corrected for Lorentz-polarization effects, for absorption[18] and also for intensity decay [Intensities of three standard reflections dropped during data collection by 26%, thus resulting in a $R_{int}$ value of 0.0480]. Crystallographic data and processing parameters are given in Table I.

The structure was solved by Patterson methods and subsequent Fourier analyses. Anisotropic displacement parameters were applied to non-hydrogen atoms in full-matrix least-squares refinements based on $F^2$. The hydrogen atoms were assigned with common isotropic displacement factors and included in the final refinement cycles by use of geometrical restraints. The programs DIFABS[18]; SHELXL-93[19], and SHELXS-86[20], both incorporated in the SHELXTL/PC[21] program package, and PLATON[22] were used for computations. Analytical expressions of neutral-atom scattering factors were employed, and anomalous dispersion corrections were incorporated[23]. Fractional atomic coordinates are listed in Table II; selected bond distances and bond angles are given in Table III. Positional parameters, anisotropic displacement parameters, hydrogen atom coordinates, a full list of bond lengths and angles and observed and calculated structure factors are available from MASG.

## RESULTS AND DISCUSSION

The reaction between manganese(II) ions and ethyl nicotinate in the presence of the azide ion in aqueous or aqueous/ethanolic media afforded the title complex. The complex is insoluble in cold water, ethanol, acetone, benzene and chloroform, but soluble in boiled water, DMF and DMSO giving rise to non-conducting solutions.

TABLE I Crystallographic data and processing parameters

| | |
|---|---|
| Molecular formula | $C_{16}H_{18}MnN_8O_4$ |
| Molecular weight | 441.32 |
| Color | light green |
| System, Space group | Monoclinic, $P2_1/c$ |
| $a$ (Å) | 15.122(4) |
| $b$ (Å) | 8.815(3) |
| $c$ (Å) | 15.170(5) |
| $\alpha$ (°) | 90 |
| $\beta$ (°) | 91.45(2) |
| $\gamma$ (°) | 90 |
| $V$ (Å$^3$), | 2022(1) |
| $Z$ | 4 |
| $\mu$(MoK$\alpha$) (mm$^{-1}$) | 0.693 |
| Normalized transmission factors | 1.000-0.459 |
| $D_{calc}/D_{obs}$ (Mg/m$^3$) | 1.450/1.46(2) |
| Approx. crystal size (mm) | 0.80 × 0.60 × 0.30 |
| 2θ range of data collection (°) | 2.97-26.49 |
| Reflections collected | 4534 |
| Independ. refl./$R_{int}$ | 3624/0.0480 |
| Parameters | 270 |
| Goodness-of-Fit on $F_o^2$ | 1.062 |
| $R_1/wR_2$ | 0.0579/0.1402 |
| Weighting factors*: a/b | 0.0887/0.0928 |
| Largest peak/hole (eÅ$^{-3}$) | 0.273/−0.586 |

*) $w^{-1} = [\sigma^2(F_o^2) + (aP)^2 + bP]$ and $P = (F_o^2 + 2F_c^2)/3$

Figures 1 and 2 illustrate the principle structural features of the $Mn(N_3)_2$(ethyl nicotinate)$_2$ complex, in which the manganese atom is located in a *trans* octahedral environment. Each manganese atom is bonded to four azido ligands and two axial ethyl nicotinate molecules. The four azido ligands behave differently: two azido groups act as $\mu(1,1)$ bridging ligands between two manganese atoms giving rise to planar centrosymmetric $Mn_2N_2$ units, and the other two azides are $\mu(1,3)$ bridging. Thus each $Mn_2N_2$ unit is linked to the four neighboring $Mn_2N_2$ units by four $\mu(1,3)$ bridging azides, forming a two-dimensional manganese azido structure. Bond parameters in the $\mu(1,1)$ units show normal values for this kind of unit: Mn(1)-N(11) = 2.229(3), Mn(1)-N(11a) = 2.231(3) Å, Mn(1)-N(11)-Mn(1a) = 102.1(1)° and Mn(1)...Mn(1a) = 3.469(2) Å. The $\mu(1,1)$ azido groups are more asymmetric [N(11)-N(12) = 1.193(4), N(12)-N(13) = 1.164(5) Å] than $\mu(1,3)$ azido ligands [N(21)-N(22) = 1.150(5) and N(22)-N(23) = 1.165(5) Å]. All azido ligands of both types, however, are linear within experimental error [N(11)-N(12)-N(13) angle = 178.4(4)° and N(21)-N(22)-N(23) angle = 177.4(4)°]. As found for other metal complexes with $\mu(1,1)$ azido ligands the shorter N-N bonds are remote from the metal atom[26-28]. The Mn-N(L) bond lengths are longer than corresponding distances reported in

TABLE II Atomic coordinates ($\times 10^4$) and equivalent isotropic displacement parameters ($Å^2 \times 10^3$). $U_{eq}$ is one third of trace of the $U_{ij}$ tensor; estimated standard deviations in parantheses).

| *Atom* | *x/a* | *y/b* | *z/c* | $U_{eq}(Å^2)$ |
|---|---|---|---|---|
| Mn(1) | 82(1) | −55(1) | 1142(1) | 37 |
| N(11) | −596(2) | 1214(4) | 48(2) | 44 |
| N(12) | −1261(2) | 1930(3) | 108(2) | 49 |
| N(13) | −1921(3) | 2599(5) | 163(3) | 86 |
| N(21) | −537(2) | 1279(5) | 2185(3) | 68 |
| N(22) | −689(2) | 2348(4) | 2587(2) | 43 |
| N(23) | −869(2) | 3403(4) | 3010(3) | 65 |
| N(1) | −1125(2) | −1633(4) | 1272(2) | 46 |
| C(1) | −1893(2) | −1037(5) | 1537(3) | 48 |
| C(2) | −2621(3) | −1903(5) | 1738(3) | 53 |
| C(3) | −2575(3) | −3447(6) | 1657(3) | 68 |
| C(4) | −1802(4) | −4088(5) | 1378(3) | 71 |
| C(5) | −1094(3) | −3151(5) | 1189(3) | 54 |
| C(6) | −3433(3) | −1156(7) | 2082(3) | 66 |
| 0(1) | −4114(2) | −1853(5) | 2194(3) | 116 |
| 0(2) | −3308(2) | 278(4) | 2268(2) | 74 |
| C(7) | −4021(3) | 1139(8) | 2669(4) | 90 |
| C(8) | −3631(4) | 2591(7) | 2955(5) | 108 |
| N(2) | 1200(2) | 1690(3) | 1145(2) | 41 |
| C(9) | 2023(2) | 1299(5) | 921(2) | 45 |
| C(10) | 2680(2) | 2328(4) | 762(2) | 42 |
| C(11) | 2498(3) | 3861(5) | 849(3) | 46 |
| C(12) | 1664(3) | 4280(4) | 1091(3) | 50 |
| C(13) | 1040(3) | 3180(4) | 1236(3) | 45 |
| C(14) | 3561(3) | 1719(6) | 501(3) | 59 |
| 0(3) | 3689(3) | 422(5) | 347(4) | 121 |
| 0(4) | 4169(2) | 2768(4) | 433(2) | 72 |
| C(15) | 5049(3) | 2230(8) | 199(5) | 104 |
| C(16) | 5705(3) | 3355(8) | 458(5) | 106 |



the structure of *trans* $[Mn(N_3)_2(3\text{-picoline})_2(H_2O)_2]$ [2.252 (27) Å][29], but comparable with those found in the structures of polymeric $[Mn(\text{picolinato})(N_3)(H_2O)]_n$ [2.278(3) Å][13], and $[Mn(4\text{-acetyl-pyridine})_2(N_3)_2]_n$ [2.291(3) Å][30].

The structure of the title complex, **1**, differs from that reported for $[Mn(4\text{-acetylpyridine})_2(N_3)_2]_n$, **2**, although **2** contains octahedrally-coordinated manganese atoms linked by four end-to-end azido ligands and two molecules of 4-acetylpyridine in *trans* arrangement. In complex **2**, each of the four azido ligands bridges two manganese atoms[30] rather than two $Mn_2N_2$ units found in complex **1**. Complex **1** also differs from the structure of $[Mn(\text{pyridine})_2(N_3)_2]_n$, which is very similar to that of complex **2**, but consists of a three-dimensional polymer[13]. The reported structural parameters for complex **3** are: Mn-N(py) =

TABLE III Selected interatomic distances (Å) and angles (deg.) for 2, with estimated standard deviations in parantheses.

| | | | |
|---|---|---|---|
| Mn(1)...Mn(1a) | 3.469(2) | Mn(1)...Mn(1b) | 6.042(3) |
| Mn(1)-N(21) | 2.199(4) | Mn(1)-N(23b) | 2.200(4) |
| Mn(1)-N(11) | 2.229(3) | Mn(1)-N(11a) | 2.231(3) |
| Mn(1)-N(2) | 2.285(3) | Mn(1)-N(1) | 2.308(3) |
| N(11)-N(12) | 1.193(4) | N(11)-Mn(1a) | 2.231(3) |
| N(12)-N(13) | 1.164(5) | N(21)-N(22) | 1.150(5) |
| N(22)-N(23) | 1.165(5) | N(23)-Mn(1c) | 2.200(4) |
| N(1)-C(5) | 1.344(5) | N(1)-C(1) | 1.345(5) |
| C(1)-C(2) | 1.381(5) | C(2)-C(3) | 1.368(7) |
| C(2)-C(6) | 1.498(6) | C(3)-C(4) | 1.375(7) |
| C(4)-C(5) | 1.389(6) | C(6)-O(1) | 1.214(5) |
| C(6)-O(2) | 1.308(6) | O(2)-C(7) | 1.463(6) |
| C(7)-C(8) | 1.469(8) | N(2)-C(9) | 1.343(4) |
| N(2)-C(13) | 1.343(5) | C(9)-C(10) | 1.372(5) |
| C(10)-C(11) | 1.385(5) | C(10)-C(14) | 1.499(5) |
| C(11)-C(12) | 1.374(5) | C(12)-C(13) | 1.375(5) |
| C(14)-O(3) | 1.184(6) | C(14)-O(4) | 1.309(5) |
| O(4)-C(15) | 1.465(6) | C(15)-C(16) | 1.450(8) |
| | | | |
| N(21)-Mn(1)-N(23b) | 98.3(2) | N(21)-Mn(1)-N(11) | 94.1(2) |
| N(23b)-Mn(1)-N(11) | 167.7(1) | N(21)-Mn(1)-N(11a) | 172.0(1) |
| N(23b)-Mn(1)-N(11a) | 89.8(1) | N(11)-Mn(1)-N(11a) | 77.9(1) |
| N(21)-Mn(1)-N(2) | 88.1(1) | N(23b)-Mn(1)-N(2) | 91.5(1) |
| N(11)--Mn(1)-N(2) | 89.4(1) | N(11a)-Mn(1)-N(2) | 92.1(1) |
| N(21)-Mn(1)-N(1) | 84.8(1) | N(23b)-Mn(1)-N(1) | 89.7(1) |
| N(11)-Mn(1)-N(1) | 90.9(1) | N(11a)-Mn(1)-N(1) | 94.9(1) |
| N(2)-Mn(1)-N(1) | 172.9(1) | N(12)-N(11)-Mn(1) | 125.6(3) |
| N(12)-N(11)-Mn(1a) | 128.0(3) | Mn(1)-N(11)-Mn(1a) | 102.1(1) |
| N(13)-N(12)-N(11) | 178.4(4) | N(22)-N(21)-Mn(1) | 156.2(3) |
| N(21)-N(22)-N(23) | 177.4(4) | N(22)-N(23)-Mn(1c) | 133.1(3) |
| C(5)-N(1)-C(1) | 116.7(4) | C(5)-N(1)-Mn(1) | 124.1(3) |
| C(1)-N(1)-Mn(1) | 118.7(3) | N(1)-C(1)-C(2) | 123.4(4) |
| C(3)-C(2)-C(1) | 119.1(4) | C(3)-C(2)-C(6) | 120.9(4) |
| C(1)-C(2)-C(6) | 120.0(4) | C(2)-C(3)-C(4) | 118.9(4) |
| C(3)-C(4)-C(5) | 119.0(4) | N(1)-C(5)-C(4) | 122.9(4) |
| O(1)-C(6)-O(2) | 125.2(5) | O(1)-C(6)-C(2) | 122.1(5) |
| O(2)-C(6)-C(2) | 112.6(4) | C(6)-O(2)-C(7) | 119.2(4) |
| C(8)-C(7)-O(2) | 106.3(5) | C(9)-N(2)-C(13) | 116.6(3) |
| C(9)-N(2)-Mn(1) | 121.1(3) | C(13)-N(2)-Mn(1) | 121.6(2) |
| N(2)-C(9)-C(10) | 123.7(4) | C(9)-C(10)-C(11) | 118.8(3) |
| C(9)-C(10)-C(14) | 117.6(4) | C(11)-C(10)-C(14) | 123.6(3) |
| C(12)-C(11)-C(10) | 118.2(4) | C(11)-C(12)-C(13) | 119.5(4) |
| N(2)-C(13)-C(12) | 123.2(4) | O(3)-C(14)-O(4) | 123.3(4) |
| O(3)-C(14)-C(10) | 123.2(4) | O(4)-C(14)-C(10) | 113.5(4) |
| C(14)-O(4)-C(15) | 115.7(4) | C(16)-C(15)-O(4) | 109.4(5) |

symmetry codes: (a) −x, −y, −z; (b) −x, y − 1/2, −z + 1/2; (c) −x, y + 1/2, −z + 1/2.

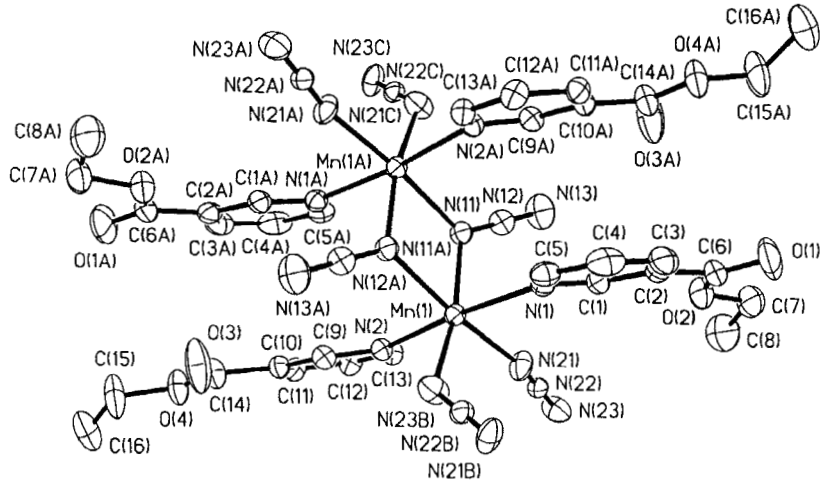


FIGURE 1 Molecular geometry and atom labelling scheme of [Mn(ethyl nicotinate)$_2$(N$_3$)$_2$]$_n$. Hydrogen atoms are omitted for clarity.

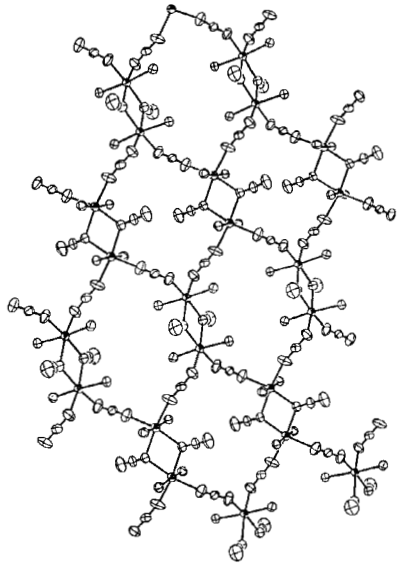

FIGURE 2 A view onto the Mn-N-sublattice of [Mn(ethyl nicotinate)$_2$(N$_3$)$_2$]$_n$. MnN$_6$ polyhedra are connected by different types of azide bridges to form a two-dimensional sheet structure.

2.259(3), Mn-$N_3$ = 2.195(5) and 2.217(4) Å, Mn-N-N = 145.4(4) and 134.1(3)°[13].

The IR and Raman spectral data for the title complex along with those of the free ligand are collected in Table IV. Both IR and Raman spectra show two bands in the region 2150-2000 $cm^{-1}$, as well as two bands in the region 1370-1250 $cm^{-1}$, associated with asymmetric and symmetrical stretching vibrations of the azido groups, respectively. For the symmetrical azide ion or azide ligand (where the two N-N distances are equal), the $\nu_{as}$ and $\delta$ modes are IR-active but Raman inactive whereas the $\nu_s$ mode is IR inactive and Raman active. The two azides in the present structure have $\Delta d$ values (the difference between two N-N distances) of 0.015 and 0.029 Å, for N(11)-N(12-N(13) and N(21)-N(22)-N(23) groups, respectively. The former azide, therefore, may be considered symmetric or very slightly asymmetric. Accordingly, a very strong IR band and a very weak or no band in the Raman spectrum due to $\nu_{as}$ mode, and an infrared band and a strong Raman line due to the $\nu_s$ mode for the slightly asymmetric azide group are expected. Figure 3(a) and (b) show the regions 2100-2000 $cm^{-1}$ and 1800-400 $cm^{-1}$ of the Raman spectrum of the title complex. It is clear that a medium band appears at 2076 $cm^{-1}$ together with a very weak line at 2030 $cm^{-1}$ and a very strong line at 1371 $cm^{-1}$ together with a medium line at 1280 $cm^{-1}$. The very weak line ($\nu_{as}$ mode) and the very strong line ($\nu_s$ mode) are due to the slightly asymmetric N(11)-N(12)-N(13) azido ligand, and the other lines are due to the other azide. According to Agrell[31] and others[32], the position of the $\nu_{as}N_3$ band depends, to the first approximation, on the degree of asymmetry of the azide group. However, while two bands due to $\nu_{as}$ $N_3$ appeared as expected, their positions in infrared and Raman spectra are not consistent with the $\Delta d$ *vs.* $\nu_{as}N_3$ relationship; according to which they should appear around 2015 and 2029 $cm^{-1}$. It is possible that the high values reflect bending of the Mn-N-N angles and their difference of about 28°. Also, it is possible that the coincidence of the vibrations related to the two azides with such similar $\Delta d$ values leads to some resonance or configuration interaction. In the far infrared region, two bands assigned as the $\nu$Mn-$N_3$ mode and one or two bands due to $\nu$Mn-N-(L) mode appeared in the infrared and Raman spectra. The stretching Mn-$N_3$ vibrations occur at 373 and 362 $cm^{-1}$ in the Raman spectrum of [Mn(bpy)$(N_3)_4$] (bpy = bipyridine) containing only terminal azido ligands[33]. With the porphirinic ligand TMP, the $\nu$Mn-$N_3$ vibration was found at 394 $cm^{-1}$ in the infrared spectrum of $N_3$Mn(III)TMP[34]. Lower frequency of the Mn-$N_3$ stretch observed in [Mn$(N_3)_2$(ethyl nicotinate)$_2]_n$ is consistent with the lower charge on the Mn atom and reflects the gradual decrease of the Mn-$N_3$ stretching vibration frequencies in the order Mn(IV) > Mn(III) > Mn(II).

TABLE IV IR and Raman spectral data ($cm^{-1}$).

| Ethyl nicotinate | | Complex | | |
|---|---|---|---|---|
| IR | Raman | IR | Raman | Assignments |
| | | 2100 s | 2076 wm | $\nu_{as}(N_3)$ |
| | | 2065 vs | 2030 vw | $\nu_{as}(N_3)$ |
| 1714 vs | 1721 m | 1720 vs | 1725 ms | $\nu_{as}(C{=}O)$ |
| | 1592 vs | 1603 m | 1604 ms | pyridine |
| 1581 m | | 1575 wm | 1587 m | pyridine |
| | | 1510 w | 1490 w | pyridine |
| 1461 wm | 1454 w | 1464 wm | 1453 w | pyridine |
| 1412 wm | 1418 vw | 1413 wm | 1427 w | pyridine |
| 1384 vw | 1395 vw | 1387 wm | 1390 w | pyridine |
| 1358 m | 1367 w | 1360 wm | 1371 vs | $\nu_s(N_3)$ |
| 1319 w | 1310 w | 1321 w | 1337 s | |
| 1284 vs | 1284 m | | 1294 ms | $\nu_s$(C00) |
| | | 1288 vs | 1280 m | $\nu_s(N_3)$ |
| 1181 w | 1196 wm | 1212 w | 1199 w | |
| 1110 vs | 1111 wm | 1133 ms | | $\nu$(CCO), $\beta$(C-H) |
| 1037 wm | 1040 vs | 1044 wm | 1050 m | $\nu_1$, ringbreathing |
| 1020 s | 1020 m | 1012 w | 1037 s | $\nu_{12}$, ring breathing |
| 850 m | 854 m | 868 w | 859 wm | |
| 740 | | 740 ms | | $\delta$(C00) |
| 700 s | 707 wm | 694 m | 708 wm | $\nu$ ring |
| 613 wm | 621 wm | 648 wm | 641 wm | $\nu$ ring |
| | | 617 | | $\delta(N_3)$ |
| | | 433 w | 431 w | $\nu$ ring |
| 395 wm | 396 vw | 415 w | 410 w | |
| | 333 m | 285 s | 338 m | $\nu$Mn-$N_3$ |
| | | 265 s | 294 wm | $\nu$Mn-$N_3$ |
| | | 240 s | 220 m | $\nu$Mn-N(L) |
| | 197 m | | 200 m | |

w = weak, m = medium, s = strong, v = very

The room temperature X-band EPR spectrum of a polycrystalline sample has been recorded. The spectrum shows a narrow intense isotropic signal centered at $g = 1.98$, accompanied by a weak hyperfine structure on both sides as seen from Figure 4(a). The peak-to-peak band width is 35 G. The $g$ value is consistent with the room temperature $g$ values of 2 found for manganese(II) azido complexes of related pyridine ligands and their magnetic properties are consistent with alternating ferro-antiferromagnetic compounds[30]. The complex dissolves in DMF and DMSO and its spectra in these solvents have been recorded; the spectrum in DMF is shown in Figure 4(b). It is clear that the isotropic signal in the solid state spectrum splits into six lines when the complex dissolves in DMF due to the hyperfine structure of $Mn^{II}$ ($I = 5/2$) with a splitting factor (A) of 91.8 G. This

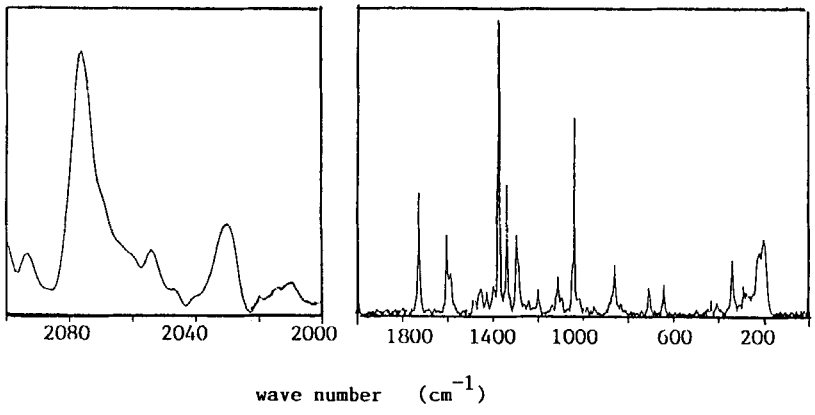


FIGURE 3 Raman spectra of [Mn(ethyl nicotinate)$_2$(N$_3$)$_2$]$_n$.



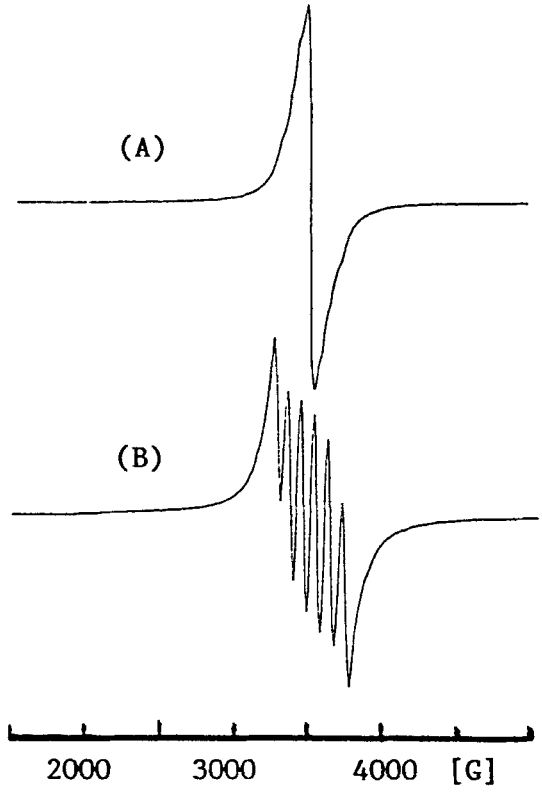


FIGURE 4 EPR spectra of the complex, (a) solid state and (b) in DMF solution.

spectrum is very similar to that of the DMSO solution and to those of hexa-coordinate manganese(II) complexes with ground state $^6S_{5/2}$[35,36].

The thermal decomposition of $[Mn(N_3)_2(\text{ethyl nicotinate})_2]_n$ complex is represented in Figure 5(a) and (b). The first step of the thermal decomposition consists of loss of one ethyl nicotinate molecule and one half of a nitrogen molecule, rather than a nitrogen atom (loss of weight (%); experimental 38.28, theoretical 37.33) around 160-170°C. This is followed immediately by loss of the

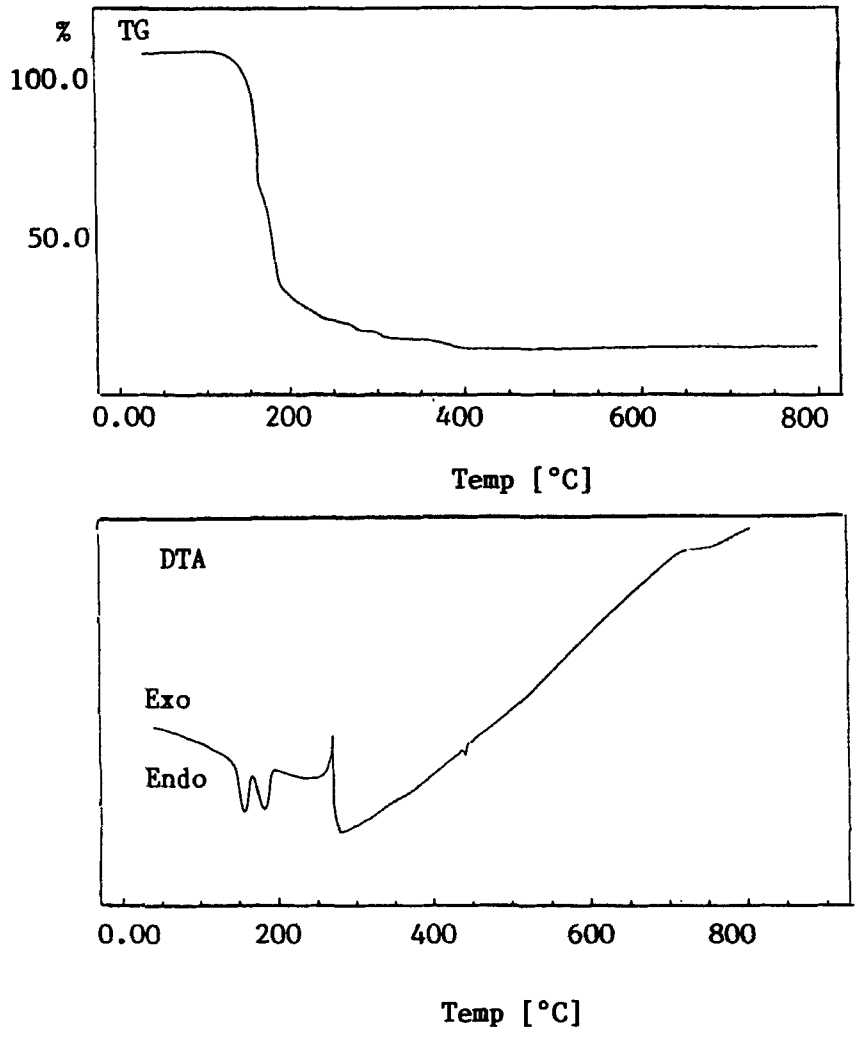


FIGURE 5 Thermal decomposition of $[Mn(\text{ethyl nicotinate})_2(N_3)_2]_n$.

second half of the nitrogen molecule, another nitrogen molecule and degradation of the carboxylate groups giving rise to $C_2H_4$ and $CO_2$ molecules. The experimental loss of weight in this stage is 25.17% whereas the theoretical is 25.85%. That there is no plateau between these two stages suggests that both are stages of one step or one process [Figure 5(a)]. The DTA curve starts this step with an endotherm ($T_{max}$ = 157° °C) followed by an immediate endotherm with a $T_{max}$ = 184°C, suggesting that they are stages of one process although these two endotherms appear as if they are well separated. The $\Delta H$ for the first endotherm is −39.5 kJ/mole and that for the second endotherm is −40.1 kJ/mole. The TG curve shows that step 2 starts immediately after the second stage of step 1, with a gradual loss of weight that reaches a value of 13.1% at 277°C. which does not reflect a simple one atage process. Although the DTA curve shows that step 2 is well separated from step 1, it shows a narrow exotherm followed immediately by an endotherm with $T_{max}$ = 275°C. The gradual loss of weight continued to reach 5.0% around 408°C, after which no loss of weight occurs till 800°C. The residue after 408°C is 18.43%, suggesting that a reductive [$Mn^{II}$-$Mn^{I}$] degradation is completed at this temperature in a dynamic nitrogen atmosphere, and a polymer residue of the empirical formula $[Mn(CN)]_n$ is indicated by the calculated weight loss of the complex.



## *Acknowledgments*

Financial support by the Kuwait University Research Administration Project (No. SC 077) and the Department of Chemistry General Faculty Projects (Analab) are gratefully acknowledged. The authors thank Prof. Kratky for the use of the STOE diffractometer.

## *References*

1. L.K. Thompson, S.S. Tandon and M.E. Manuel, *Inorg. Chem.*, **34**, 2356 (1995), and references therein.
2. A. Escuer, R. Vicente, J. Ribas and X. Solans, *Inorg. Chem.*, **34**, 1793 (1995), and references therein.
3. A. Escuer, R. Vicente, J. Ribas, M.S. El Fallah, X. Solans and M. Font-Bardia, *Inorg. Chem.*, **32**, 3727 (1993).
4. A. Escuer, R. Vicente, J. Ribas, M.S. El-Fallah, X. Solans and M. Font-Bardia, *Inorg. Chem.*, **33**, 1842 (1993).
5. J. Ribas, M. Monfort, C. Bastos, C. Diaz and X. Solans, *Inorg. Chem.*, **32**, 3557 (1993).
6. R. Vicente and A. Escuer, *Polyhedron*, **14**, 2133 (1995).
7. S. Sikorav, I. Bkouche-Waksman and O. Kahn, *Inorg. Chem.*, **23**, 490 (1984).
8. J. Comarmond, P. Plumere, J.M. Lehn, Y. Agnus, R. Louis, R. Weiss, O. Kahn and J. Norgenstern-Badarau, *J. Am. Chem. Soc.*, **104**, 6330 (1982).
9. M.F. Charlot, O. Kahn, M. Chaillet and C. Larrieu, *J. Am. Chem. Soc.*, **24**, 2574 (1986).
10. J. Ribas, M. Monfort, C. Diaz, C. Bastos and X. Solans, *Inorg. Chem.*, **33**, 484 (1994).

11. M.A.S. Goher and F.A. Mautner, *Polyhedron*, **12**, 1863 (1993).
12. M.A.S. Goher, F.A. Mautner and A. Popitsch, *Polyhedron*, **12**, 2557 (1993).
13. M.A.S. Goher, M.A.M. Abu-Youssef, F.A. Mautner and A. Popitsch, *Polyhedron*, **11**, 2137 (1992).
14. M.A.S. Goher, and F.A. Mautner, *Croat. Chem. Acta*, **63**, 559 (1990).
15. R. Cortes, L. Pizarro, L. Lazema, M. Arriortua and T. Rojo, *Inorg. Chem.*, **33**, 2697 (1994).
16. R. Cortes, L. Lazema, J.L. Pizarro, M.I. Arriortua, X. Solans and T. Rojo, *Angew. Chem. Int. Ed. Eng.*, **33**, 2488 (1994).
17. M.A.S. Goher, R.J. Wang and T.C.W. Mak, *J. Coord. Chem.*, **38**, 151 (1996).
18. N. Walker and D. Stuart, *Acta Cryst.*, A39, 158 (1983).
19. G.M. Sheldrick, "SHELXL-93" (Universität Göttingen, Germany, 1993),
20. G.M. Sheldrick, "SHELXS-86" (Universität Göttingen, Germany, 1986).
21. SHELXTL/PC v.5.03, Siemens Analytical Automation Inc., Madison, WI (1995).
22. A.L. Spek, in Computational Crystallography (Edited by D. Sayre), (Clarendon Press, Oxford, 1982), p. 528.
23. International Tables for Crystallography, Vol. C, (Edited by A.J.C. Wilson), (Kluwer Academic Publishers, Dordrecht, 1992), Tables 4.2.6.8 and 6.1.1.4.
24. M.A.S. Goher and M.A.M. Abu-Youssef, *Acta Chim Hung.*, **124**, 749 (1987).
25. B.N. Figgis and J. Lewis, *Progr. Inorg. Chem.*, **4**, 959 (1964)
26. Z. Dori and R.F. Ziolo, *Chem. Rev.*, **73**, 247 (1973).
27. I. Agrell, *Acta Chem. Scand.*, **24**, 1247 (1970); I. Agrell and N. Vannerberg, *ibid.*, **25**, 1639 (1971); I. Agrell, *ibid.*, **24**, 3575 (1970).
28. M.A.S. Goher and T.C.W. Mak, *Inorg. Chim. Acta*, **85**, 215 (1984); *ibid.*, **89**, 119 (1984); T.C.W. Mak and M.A.S. Goher, *Inorg. Chim. Acta*, **115**, 17 (1986); M.A.S. Goher, M.A.M. Abu-Youssef and F.A. Mautner, *Z. Naturforsch.*, **47b**, 139 (1992).
29. F.A. Mautner and M.A.S. Goher, *Cryst. Res. Technol.*, **25**, 1271 (1990).
30. A. Escuer, R. Vicente, M.A.S. Goher and F.A. Mautner, *Inorg. Chem.*, **34**, 5707 (1995); *ibid.*, **35**, 6386 (1996), and references therein.
31. I. Agrell, *Acta Chem. Scand.*, **25**, 2965 (1971).
32. M.A.S. Goher, *Acta Chim. Hung.*, **127**, 213 (1990).
33. B.C. Dave and R.S. Czernuszewicz, *J. Coord. Chem.*, **33**, 257 (1994).
34. R.S. Czernuszewicz, W.F. Wadner, G.B. Ray and K. Nakamoto, *J. Mol. Struct.*, **242**, 99 (1991).
35. B.R. Srinivasan and S. Saker, *Inorg. Chem.*, **29**, 3898 (1990).
36. T.S. Lobana and N. Bala, *Trans. Metal Chem.*, **19**, 115 (1994); G. Batre and P. Mathur, *Trans. Metal. Chem.*, **19**, 160 (1994).